Structure, Function, and Stability of Enzymes Covalently Attached to Single-Walled Carbon Nanotubes

ARTICLE *in* LANGMUIR · DECEMBER 2007

Impact Factor: 4.46 · DOI: 10.1021/la702091c · Source: PubMed

6 AUTHORS, INCLUDING:

Prashanth Asuri
Santa Clara University
31 PUBLICATIONS **1,074** CITATIONS
SEE PROFILE

Shyam Sundhar Bale
Massachusetts General Hospital
42 PUBLICATIONS **857** CITATIONS
SEE PROFILE

Ravindra Pangule
Regeneron Pharmaceuticals Inc.
15 PUBLICATIONS **802** CITATIONS
SEE PROFILE

Dhiral A Shah
Sanofi Aventis Group
8 PUBLICATIONS **218** CITATIONS
SEE PROFILE

Structure, Function, and Stability of Enzymes Covalently Attached to Single-Walled Carbon Nanotubes

Prashanth Asuri, Shyam Sundhar Bale, Ravindra C. Pangule, Dhiral A. Shah, Ravi S. Kane,* and Jonathan S. Dordick*

Department of Chemical and Biological Engineering, Center for Biotechnology & Interdisciplinary Studies, Rensselaer Nanotechnology Center, Rensselaer Polytechnic Institute, Troy, New York 12180

Received July 12, 2007. In Final Form: August 28, 2007

We describe the structure, activity, and stability of enzymes covalently attached to single-walled carbon nanotubes (SWNTs). Conjugates of SWNTs with three functionally unrelated enzymes—horseradish peroxidase, subtilisin Carlsberg, and chicken egg white lysozyme—were found to be soluble in aqueous solutions. Furthermore, characterization of the secondary and tertiary structure of the immobilized proteins by circular dichroism and fluorescence spectroscopies, respectively, and determination of enzyme kinetics revealed that the enzymes retained a high fraction of their native structure and activity upon attachment to SWNTs. The SWNT−enzyme conjugates were also more stable in guanidine hydrochloride (GdnHCl) and at elevated temperatures relative to their solution counterparts. Thus, these protein conjugates represent novel preparations that possess the attributes of both soluble enzymes—high activity and low diffusional resistance—and immobilized enzymes—high stability—making them attractive choices for applications ranging from diagnostics and sensing to drug delivery.

Introduction

Progress in the controlled synthesis and functionalization of nanomaterials, in particular carbon nanotubes, has impacted numerous applications ranging from sensing[1−3] to delivery[4−6] and the design of functional composites.[7−9] Many of these applications rely on interfacing proteins with carbon nanotubes and require that the proteins retain their native structure and activity on the nanoscale support.[1−4,9−15] As a result, the attachment of proteins to carbon nanotubes has been well-studied, and a variety of both covalent[3−5,16] and noncovalent methods[1,2,10−14] have been explored to attach proteins onto carbon nanotubes. Despite this considerable progress in the preparation of nanotube−protein conjugates, few studies have yielded detailed information on the structure and function of proteins attached to nanotubes.[10,11]

Here, we report the generation of water-soluble conjugates of single-walled carbon nanotubes (SWNTs) with a range of enzymes differing significantly in both structure and function. Attachment onto SWNTs results in high loadings (up to 1.3 mg/mg of SWNT) of functional water-soluble enzyme preparations. This solubility and high enzyme loading enables a detailed spectroscopic characterization of protein structure to be performed, which complements kinetic analyses of activity and stability. These studies demonstrate the enhanced stability of SWNT−enzyme preparations relative to free enzymes in solution. Such water-soluble, structurally characterized enzyme−nanotube conjugates may be useful in applications where a high density of processible biocatalysts is required, e.g., biosensors, active biocatalytic paints and coatings, and biotransformations.

Experimental Section

Materials. Horseradish peroxidase (HRP), subtilisin Carlsberg (SC), chicken egg white lysozyme, soybean peroxidase (SBP), *N*-succinyl-L-Ala-L-Ala-L-Pro-L-Phe-*p*-nitroanilide (AAPF-NA), 2,2′-azinobis(3-ethylbenzthiazoline-6-sulfonic acid) (ABTS), and *Micrococcus lysodeikticus* cells were purchased from Sigma (St. Louis, MO) as salt-free, dry powders and were used without further purification. Raw SWNTs were purchased from Carbon Nanotechnologies, Inc. (Houston, TX). Guanidine hydrochloride (GdnHCl) and all other chemicals were purchased from Sigma and used as received.

Acid Treatment of SWNTs. As-received SWNTs (100 mg) were suspended in 400 mL of a mixture of concentrated sulfuric acid and nitric acid (3:1, v/v) and bath sonicated for 3 h. The nanotube suspension was diluted with MilliQ water and washed with copious amounts of water by filtering through a 0.2 μm polycarbonate membrane. The nanotube film thus formed was resuspended in water by ultrasonication and filtered again to remove the acid. The ultrasonication/filtration step was repeated at least three times until water-soluble nanotubes were obtained.

Enzyme Attachment onto Nanotubes. The acid-treated SWNTs (1 mg/mL) dispersed in MES [2-(*N*-morpholino)ethanesulfonic acid] buffer (50 mM, pH 6.2) were added to an equal volume of 400 mM

* Corresponding authors. E-mail: dordick@rpi.edu (J.S.D.), kaner@rpi.edu (R.S.K.).

(1) Barone, P. W.; Baik, S.; Heller, D. A.; Strano, M. S. *Nat. Mater.* **2005**, *4,* 86.
(2) Chen, R. J.; Bangsaruntip, S.; Drouvalakis, K. A.; Kam, N. W. S.; Shim, M.; Li, Y.; Kim, W.; Utz, P. J.; Dai, H. *Proc. Natl. Acad. Sci. U.S.A.* **2003**, *100*, 4984.
(3) Besteman, K.; Lee, J. O.; Wiertz, F. G. M.; Heering, H. A.; Dekker, C. *Nano Lett.* **2003**, *3*, 727.
(4) Kam, N. W. S.; Jessop, T. S.; Wender, P. A.; Dai, H. *J. Am. Chem. Soc.* **2004**, *126*, 6850.
(5) Pantarotto, D.; Briand, J.-P.; Prato, M.; Bianco, A. *Chem. Commun.* **2004**, 16.
(6) Kam, N. W. S.; O'Connell, M.; Wisdom, J. A.; Dai, H. *Proc. Natl. Acad. Sci. U.S.A.* **2005**, *102,* 11600.
(7) Rege, K.; Raravikar, N. R.; Kim, D.−Y.; Schadler, L. S.; Ajayan, P. M.; Dordick, J. S. *Nano Lett.* **2003**, *3*, 829.
(8) Graff, R. A.; Swanson, J. P.; Barone, P. W.; Baik, S.; Heller, D. A.; Strano, M. S. *Adv. Mater.* **2005**, *17*, 980.
(9) Asuri, P.; Karajanagi, S. S.; Kane, R. S.; Dordick, J. S. *Small* **2007**, *3*, 50.
(10) Karajanagi, S. S.; Vertegel, A. A.; Kane, R. S.; Dordick, J. S. *Langmuir* **2004**, *20*, 11594.
(11) Asuri, P.; Karajanagi, S. S.; Yang, H.; Yim, T.−J.; Kane, R. S.; Dordick, J. S. *Langmuir* **2006**, *22*, 5833.
(12) Erlanger, B. F.; Chen, B.-X.; Zhu, M.; Brus, L. *Nano Lett.* **2001**, *1*, 465.
(13) Shim, M.; Kam, N. W. S.; Chen, R. J.; Li, Y.; Dai, H. *Nano Lett.* **2002**, *2,* 285.
(14) Panhius, M.; Salvador-Morales, C.; Franklin, E.; Chambers, G.; Fonseca, A.; Nagy, J. N.; Blau, W. J.; Minett, A. I. *J. Nanosci. Nanotechnol.* **2003**, *3*, 209.
(15) Asuri, P.; Karajanagi, S. S.; Dordick, J. S.; Kane, R. S. *J. Am. Chem. Soc.* **2006**, *128*, 1046.
(16) Asuri, P.; Karajanagi, S. S.; Sellito, E.; Kim, D.−Y.; Kane, R. S.; Dordick, J. S. *Biotechnol. Bioeng.* **2006**, *95*, 804.

10.1021/la702091c CCC: $37.00
Published on Web 10/18/2007

N-hydroxysuccinimide (NHS) in MES buffer. The mixture was sonicated for 30 min followed by addition of 20 mM *N*-ethyl-*N*′-(3-(dimethylamino)propyl)carbodiimide hydrochloride (EDC) to initiate the coupling of NHS to the carboxylic groups on the oxidized nanotubes. The resulting mixture was stirred at 200 rpm for 30 min. The activated nanotube solution was then filtered through a polycarbonate membrane (0.2 μm) and rinsed thoroughly with MES buffer to remove excess EDC and NHS. The nanotube film was transferred to a solution of enzyme (10 mg/mL, 10 mM phosphate buffer, pH 8.0) and sonicated for ca. 1 min to redisperse the nanotubes. The mixture was then shaken at room temperature on an orbital shaker at 200 rpm during the conjugation of enzymes to nanotubes. The nanotube−enzyme suspension was then filtered (0.2 μm polycarbonate membrane) and washed three times with water and once with 1% Tween-20 to remove any nonspecifically adsorbed enzyme. Control nanotube−enzyme conjugates were prepared using an identical procedure, only without using EDC and NHS. The amount of immobilized enzyme was determined by elemental analysis (Atlantic Micro Lab, Inc., Norcross, GA) of the acid-treated nanotubes and the SWNT−enzyme conjugates.

Determination of Enzyme Activity. The activity of HRP was measured using ABTS as the substrate. HRP catalyzes the oxidation of ABTS in the presence of hydrogen peroxide (H_2O_2) to form a soluble product whose concentration can be quantified by measuring its absorbance at 412 nm. The activity of SC was measured using AAPF-NA as the substrate. SC catalyzes the hydrolytic cleavage of AAPF-NA, releasing the chromophore, *p*-nitroaniline, which absorbs at 405 nm. The activity of lysozyme was determined by following the lysis of *M. lysodeikticus* cells, which is quantified by monitoring the decrease in turbidity at 450 nm as a function of time. All kinetic measurements were made using a Shimadzu UV-2401 PC spectrophotometer (Columbia, MD).

Circular Dichroism Spectroscopy. The secondary structure of HRP and the SWNT−HRP conjugates was monitored by circular dichroism (CD) spectroscopy. The far-UV CD spectra (200−250 nm) of the native and immobilized enzymes were recorded on an OLIS DSM-10 CD instrument (Bogard, GA) at 20 °C using cylindrical quartz cuvettes with a 1-cm path length. In all measurements, the protein concentration was 50 μg/mL. CD spectra of the oxidized SWNTs (50 μg/mL) were recorded similarly as a control. At least three CD spectra were acquired for each sample. The spectra were then averaged and the α-helix content was calculated on the basis of the mean residue ellipticity at 222 nm (θ_{222}). For denaturant unfolding studies, protein solutions were equilibrated in solutions of GdnHCl for 24 h at room temperature prior to data acquisition. For thermal unfolding studies, the temperature was increased from 20 to 99 °C with a heating rate of 0.5 °C/min. To determine enzyme deactivation at elevated temperatures, the enzyme conjugates were exposed to a given temperature for different periods of time and cooled to room temperature in an ice bath. Initial rates were then measured at room temperature to give irreversible denaturation rate constants.

Tryptophan Fluorescence. The tertiary structure of HRP and SWNT−HRP conjugates was characterized by tryptophan fluorescence measurements. The fluorescence measurements were carried out using a Shimadzu RF-5000 spectrofluorometer (Columbia, MD). The fluorescence intensity and λ_{max} of emission of tryptophan residues within the native and immobilized HRP was measured after excitation at 283 nm. In all measurements, the protein concentration was 36 μM. L-Tryptophanamide (36 μM) was used as a control to measure the fluorescence of non-protein-containing tryptophan. Peroxidase conjugates or L-tryptophanamide was equilibrated in solutions of GdnHCl for 24 h at room temperature prior to spectral measurements. Fluorescence spectra of the solvents were subtracted from the spectra of enzyme or L-tryptophanamide.

Results and Discussion

The processing and ultimate practical use of enzyme−nanotube conjugates requires high enzyme loading and solubility while near native catalytic activity and high stability are maintained.

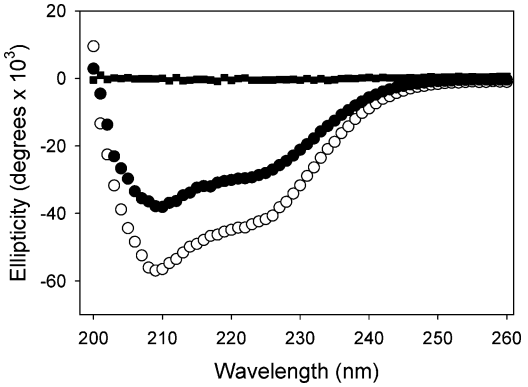

Figure 1. Far-UV CD spectra of native HRP (○), HRP attached to SWNTs (●), and bare SWNTs (control, ■).

Table 1. Loading and Relative Activity and Structure of Water-Soluble SWNT−enzyme Conjugates

enzyme	loading (mg/mg)	relative activity[a] (%)	relative structure[b] (%)
HRP	1.3	49 ± 5	68 ± 4
SC	1.3	53 ± 4	76 ± 3
Lyz	1.2	43 ± 6	63 ± 3

[a] The relative activity for different enzymes was calculated as (specific activity of enzyme−SWNT conjugate/specific activity for native enzyme) × 100. [b] The relative structure for different enzymes (except SC) was calculated as (θ_{222} for enzyme−SWNT conjugate/θ_{222} for native enzyme) × 100. SC is primarily a β-sheet protein, and its relative structure was calculated at 218 nm.

Since every atom in a SWNT is surface exposed, we reasoned that high enzyme loadings could be achieved using this nanoscale material. To that end, we covalently attached a model enzyme, horseradish peroxidase, to SWNTs. The enzyme was attached onto the surface of acid-oxidized SWNTs using carbodiimide activation of the nanotube-bound carboxylic acid groups (see the Experimental Section). Standard kinetic assays suggested that HRP retained a high percentage of its native solution activity (Table 1). The control sample (HRP exposed to oxidized SWNTs in the absence of EDC and NHS) showed <5% of the activity of the covalently attached SWNT−HRP conjugate, suggesting that the nonspecific adsorption of HRP onto oxidized SWNTs was minimal. In addition, the high support surface area facilitated high enzyme loadings (up to 1.3 mg of HRP/mg of SWNT) as determined by elemental analysis. The amount of enzyme loaded was ca. 8-fold higher than on multiwalled carbon nanotubes (MWNTs). We reasoned that these high enzyme loadings would enable us to perform spectroscopic analysis of protein structure on the SWNT conjugates; such studies were not possible with MWNT−enzyme conjugates due to interference by the nanotubes at low protein loadings.[11]

We used CD spectroscopy to assess the impact of covalent attachment on the secondary structure of HRP. To quantify the enzyme's α-helix content, we measured the mean residue ellipticity at 222 nm. Figure 1 shows CD spectra of native HRP, SWNT−HRP conjugates, and oxidized SWNTs. We note that bare oxidized SWNTs did not contribute to the SWNT−HRP conjugate spectrum. HRP attached to SWNTs retains 68% of its native α-helix content (Table 1); this value is similar to that for the related enzyme soybean peroxidase, which retains 77% of its native α-helix content when noncovalently adsorbed onto SWNTs.[10] This retention of secondary structure and activity when attached to SWNTs is not unique to peroxidases. When the hydrolytic enzymes subtilisin and lysozyme were covalently attached to SWNTs, loadings of at least 1.2 mg of protein/mg

of SWNT were obtained and activities of at least 40% of that observed in aqueous solutions were achieved (Table 1). Finally, as with HRP, a significant percentage of secondary structure was retained following covalent attachment of these enzymes onto SWNTs (Table 1). For SC, which is primarily a β-sheet protein, its secondary structure was quantified by measuring the mean residue ellipticity at 218 nm.

Having established the retention of enzyme activity and structure following covalent attachment to SWNTs, we proceeded to examine the intrinsic stability of the enzyme. To that end, we tested the effect of GdnHCl and elevated temperature on the unfolding of native HRP and SWNT−HRP conjugates by using CD spectroscopy. HRP is known to undergo a two-state transition from the native state, N, to the denatured, unfolded state, U (N ↔ U).[17] This equilibrium between the native and denatured states may be described by an equilibrium constant, K, which is related to the fraction of protein present in the unfolded state (f_U)[18] such that

$$K = \frac{f_U}{f_N} = \frac{f_U}{1 - f_U} \tag{1}$$

where f_N represents the fraction of protein present in the native state and f_U may be calculated by the following equation

$$f_U = \frac{S_N - S}{S_N - S_U} \tag{2}$$

where S is the observed CD signal (222 nm) at a given GdnHCl concentration, and S_N and S_U represent the CD signals (222 nm) for the native and unfolded conformations, respectively.

The equilibrium constant, K, is related to the Gibbs free energy of denaturation (ΔG_d) by eq 3.

$$\Delta G_d = -RT \ln K \tag{3}$$

The value of ΔG_d depends linearly on the denaturant concentration for a two-state denaturation model.[19] This relationship

$$\Delta G_d = \Delta G(H_2O) - m[\text{GdnHCl}] \tag{4}$$

can be extrapolated to determine $\Delta G(H_2O)$, the value of ΔG_d in the absence of the denaturant, which defines the conformational stability of proteins.[20,21] The additional factor m in eq 4 is an experimental measure of the dependence of ΔG_d on denaturant concentration and is related to the difference in solvent-accessible surface areas of the unfolded and folded states of the protein.

Figure 2a represents typical GdnHCl-induced unfolding curves of the two HRP preparations. The nanoscale conjugates exhibit higher tolerance toward GdnHCl than native enzyme. The denaturation curves were analyzed using eqs 1−3 to obtain ΔG_d, which was then plotted against the concentration of GdnHCl to obtain the observed unfolding transition midpoint concentration, C_m (at $\Delta G_d = 0$), and the intrinsic unfolding free energy of HRP, $\Delta G(H_2O)$. As shown in Figure 2b and Table 2, the C_m for HRP in GdnHCl increased from 1.6 M for native HRP to 2.4 M for SWNT−HRP conjugates. Furthermore, the value of $\Delta G(H_2O)$ increases from ca. 19 kJ/mol for native HRP to 26 kJ/mol for SWNT−HRP conjugates, indicating a greater stability of HRP on SWNTs relative to the native enzyme (Table 2). Interestingly,

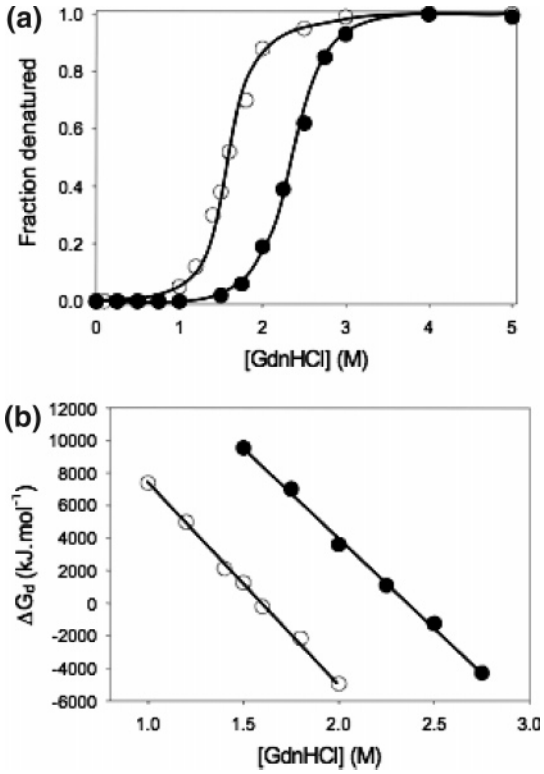

Figure 2. (a) Fraction of HRP denatured determined by measuring α-helicity at 222 nm and (b) Gibbs free energy of denaturation (ΔG_d) as a function of GdnHCl concentration: native HRP (○) and SWNT−HRP conjugates (●). The concentration of the denaturant was gradually increased from 0 to 5 M.

Table 2. Thermodynamic Parameters[a] Derived from the Unfolding Curves of Native and Immobilized HRP Using Eqs 1−3

probe	ΔC_m (M)	$\Delta\Delta G(H_2O)$ (kJ mol^{-1})
near-UV CD	0.8	6.6
fluorescence	0.7	6.7
probe	ΔT_m (°C)	$\Delta\Delta G(H_2O)$ (kJ mol^{-1})
near-UV CD	13	NA[b]

[a] C_m, T_m, and $\Delta G(H_2O)$ of native HRP were subtracted from the corresponding values for SWNT−HRP to calculate ΔC_m, ΔT_m, and $\Delta\Delta G(H_2O)$ respectively. [b] Thermal denaturation represents an irreversible process and therefore cannot be analyzed using a two-state model to calculate $\Delta G(H_2O)$.

the m values are similar for native HRP and SWNT−HRP (similar slopes in Figure 2b), consistent with protein stabilization by SWNTs without significant differences in the change of solvent-accessible surface area during protein unfolding.

To complement the CD experiments, we conducted fluorescence measurements to investigate the effect of GdnHCl on the tertiary structure of HRP in its native and immobilized forms. The polarity and charge densities surrounding tryptophan residues influence both the fluorescence intensity and maximal emission wavelength (λ_{max}). Upon protein denaturation, the quantum yield and tryptophan emission wavelength tend toward those of free tryptophan in solution; structural changes can thus be inferred from alteration of the tryptophan's microenvironment as determined by fluorescence spectroscopy. HRP possesses a single buried tryptophan residue at position 117,[22] which simplifies interpretation of fluorescence changes in the protein and allows

(17) Moosavi-Movahedi, A. A.; Nazari, K. *Int. J. Biol. Macromol.* **1995**, *17*, 43.
(18) Pace, C. N. *Crit. Rev. Biochem.* **1975**, *3*, 1.
(19) Pace, C. N.; Shaw, K. L. *Proteins* **2000**, *4*, 1.
(20) Knapp, J.; Pace, C. N. *Biochemistry* **1974**, *13*, 1289.
(21) Pace, C. N. *Methods Enzymol.* **1986**, *13*, 266.

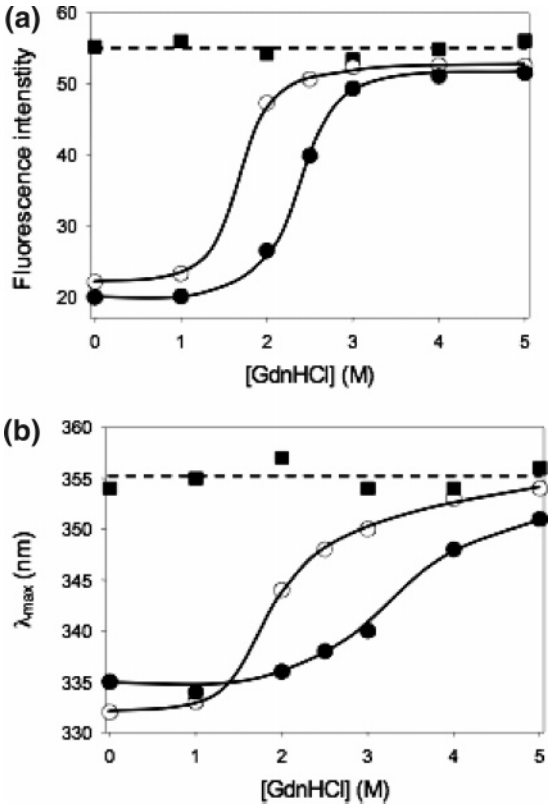

Figure 3. (a) Florescence intensity (excitation at 283 nm and emission at λ_{max}) and (b) λ_{max} of L-tryptophanamide (■), native HRP (○), and SWNT−HRP (●) as a function of GdnHCl concentration.

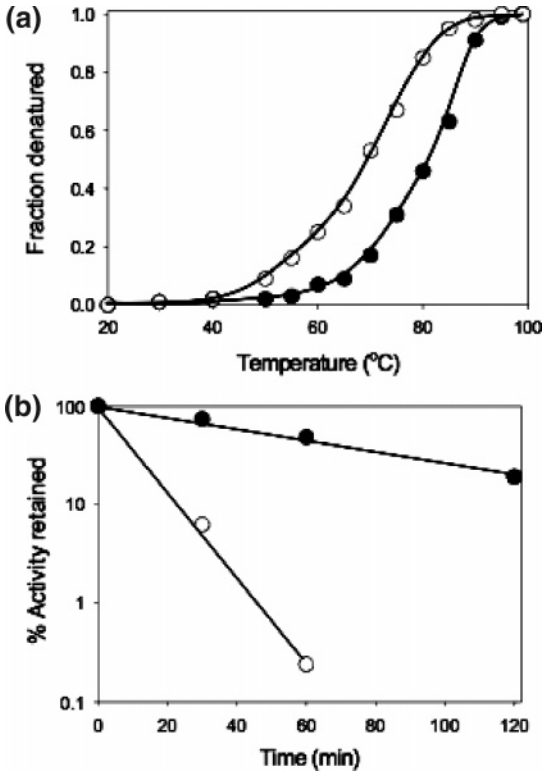

Figure 4. (a) Fraction of HRP denatured determined by measuring α-helicity at 222 nm: native HRP (○) and SWNT−HRP (●). The temperature was gradually raised from 25 to 99 °C at 0.5 °C/min. (b) Time-dependent deactivation of HRP at 90 °C: native HRP (○) and SWNT−HRP (●).

more direct correlation of fluorescence changes to bulk tertiary changes on the protein.[22,23]

As shown in Figure 3, at lower concentrations of GdnHCl, the fluorescence intensity and λ_{max} of both native HRP and SWNT−HRP conjugates were lower than those of free L-tryptophanamide, as expected for a buried tryptophan residue.[22,23] However, at higher concentrations of GdnHCl, both the intensity and λ_{max} for the native enzyme increased toward those of free L-tryptophanamide, indicating that the HRP's tryptophan residue was now more accessible to the solvent and the enzyme underwent some degree of denaturation under these conditions. The SWNT−HRP conjugates were more tolerant to the changes in GdnHCl concentration, as reflected in a more gradual increase in fluorescence intensity and λ_{max} as GdnHCl concentration was increased. Interestingly, the C_m and $\Delta G(H_2O)$ values for native HRP and SWNT−HRP conjugates were nearly identical to those obtained by CD (see above). This similarity suggests that concerted changes in HRP's secondary and tertiary structure occur during unfolding in the presence of GdnHCl. In combination, the results obtained from CD spectroscopy and fluorescence measurements indicate that SWNT−HRP conjugates are more stable under denaturing conditions than native HRP.

The enhancement in stability for the SWNT−HRP conjugates was also observed under thermal denaturation conditions, which represents an irreversible denaturation process. Figure 4a shows typical thermal denaturation curves of native HRP and SWNT−HRP. The values of the apparent unfolding transition midpoint, T_m, increased from ca. 79 °C (for native HRP) to 92 °C after covalent attachment to SWNTs, thereby indicating thermostabilization of HRP by conjugation to SWNTs. Consistent with this thermostabilization, the SWNT−HRP conjugates have a half-life ($\tau_{1/2}$) of ca. 52 min at 90 °C, 7-fold higher than that of the native enzyme ($\tau_{1/2}$ = 7 min) (Figure 4b). These results indicate a significant enhancement in stability in harsh environments for HRP attached to SWNTs.

Conclusions

In conclusion, we demonstrate that acid-treated SWNTs represent exciting materials for the preparation of enzyme conjugates with high active-enzyme loadings per unit weight of the material. High active loading of enzymes onto the nanotubes allowed for characterization using CD spectroscopy and tryptophan fluorescence in conjunction with kinetic assays, which confirmed that a variety of enzymes retained a high fraction of their native activity and structure when attached to SWNTs. Furthermore, these studies also revealed the enhanced stability of enzymes attached to SWNTs under denaturing environments relative to native enzymes. Indeed, to our knowledge, this is the first thermodynamic analysis of protein stabilization by covalent attachment onto SWNTs. Finally, this study provides a novel route to prepare water-soluble enzyme conjugates with high activity and stability for applications in sensing, self-assembly, and biomaterials.

Acknowledgment. The authors thank Dr. Wilfredo Colón, Virginia Muniz, Dr. Wen Shang, and Joe Nuffer for their guidance and assistance with CD spectroscopy. This work was supported by the NSF-NSEC (DMR-0117792) and the NIH (DE017213).

LA702091C

(22) Welinder, K. G. *Eur. J. Biochem.* **1979**, *96*, 483.
(23) Ryu, K.; Dordick, J. S. *Biochemistry* **1992**, *31*, 2588.